

## Impact of electric vehicle charging synchronization on the urban power distribution network of Frederiksberg

Tim Unterluggauer<sup>1</sup>, Sergey Klyapovskiy<sup>1</sup>, F. Hipolito<sup>2</sup>, Peter Bach Andersen<sup>1</sup>

<sup>1</sup>*Department of Wind and Energy Systems, Technical University of Denmark, 2800 Kgs. Lyngby, Denmark. Email: {timun, seklya, pba}@dtu.dk*

<sup>2</sup>*Department of Management Engineering, Technical University of Denmark, DTU 2800 Kgs. Lyngby, Denmark. Email: fabhi@dtu.dk*

---

### Executive Summary

The uptake of electric vehicles (EVs) may pose a challenge to power distribution networks (PDNs). While smart charging can be deployed to optimize charging regarding different objectives, it can exacerbate peak power demand due to synchronization. We assess the charging demand emerging from a large fleet of EVs, with models for the decision to charge and distribution of the steady-state state-of-charge. These are applied to the municipality of Frederiksberg, Denmark, using data from the national travel survey. Home and workplace charging is mapped to the PDN considering different behaviours and degrees of synchronization. Results indicate that the likelihood of severe congestion in the medium voltage PDN is low, and that it can be attributed to rare scenarios in which high synchronization is observed, particularly when maintaining the normal steady-state demand. Despite the low likelihood, preventive measures should be devised to mitigate such scenarios, especially if additional high-power consumers are connected.

*Keywords:* charging, demand, energy network, EV, simulation

---

## 1 Introduction

Electrification of road transport, particularly personal vehicle utilization, has been identified as an important means to address the global challenge of reducing carbon emissions [1]. The growth of EV market share has stimulated extensive research on the analysis of the impact of uncontrolled charging in PDNs and in the use of smart charging to mitigate this risk [2, 3, 4]. However, recent studies show that the coincidence factor (CF) of uncontrolled charging with increasing fleet size and charging power is expected to be rather low, typically less than 25% [5, 6]. In contrast, little attention has been dedicated to the analysis of unintended consequences of smart charging, namely the risks posed by the synchronization of charging to external signals, such as electricity price variations, carbon emission minimization, or the provision of ancillary services. Existing literature [7, 8] indicates that cost minimization could be a driving force for undesirable synchronization effects in home charging.

In this paper, we address the potential impact of charging synchronization by comparing different EV charging scenarios, where smart charging is considered for home and workplace charging due to the high EV flexibility potential associated with such charging events [9]. Five base scenarios  $S_i$  for EV charging are devised to analyse the impact of a fully electrified fleet of personal vehicles on a real medium voltage PDN, namely:  $S_1$ ) uncontrolled non-daily charging,  $S_2$ ) uncontrolled daily charging,  $S_3$ ) time-synchronized non-daily charging,  $S_4$ ) time-synchronized daily charging, and  $S_5$ ) time-and day-synchronized non-daily charging. The first and second scenarios concern unconstrained charging, in

which no management is imposed on the charging process and the EVs charge upon arrival.  $S_1$  sets a baseline for the charging demand, in which drivers charge  $\delta\varepsilon$  with a mean interval of  $d_p$  days, according to the decision model and steady-state demand introduced in Ref. [10]. In this scenario, only a subset of EVs charge on a given day, as determined by the aforementioned decision model. In contrast,  $S_2$  probes the impact of satisfying the energy demand on a daily basis, i.e. charging  $\delta\varepsilon/d_p$  every day. The impact of smart charging coordination at a specific time of the day is addressed in the remaining scenarios. Scenarios  $S_3$  and  $S_4$  are defined as  $S_1$  and  $S_2$ , but charging is only allowed to start, if altogether possible, after the coordination signal time. Finally,  $S_5$  simulates an extreme demand case, where all EVs must charge their steady-state demand  $\delta\varepsilon$  on the same day.

This paper focuses its analysis on the municipality of Frederiksberg, the inner part of the metropolitan area of the city of Copenhagen (Denmark). Due to its high population density and heterogeneous combination of charging demand, it is a good case study for assessing the impact of EV adoption on the power grid in the urban context. This municipality is currently part of a comprehensive project, FUSE [11], dedicated to analyse the impacts of the electrification of private road transport, both from the perspective of transport demand and from the power grid supply standpoint. By combining real data from user behaviour, baseline power consumption in the PDN, and its topology, we offer a practical approach to analyse power grid utilization in real-world scenarios. This approach addresses the lack of real-world case studies that consider simultaneously the transportation and power distribution perspectives [12], and aims at assisting distribution system operators (DSOs) to understand the potential impact of high charging synchronization in urban areas.

The subsequent parts of this paper are organized as follows: Section 2 provides an overview of the methodology introduced in this paper; Sections 3 and 4 present and discuss the key findings; and finally, conclusions are addressed in Section 5.

## 2 Methodology

An overview of the methodology of this paper is illustrated in Fig. 1 and consists of five steps, to be discussed in the following. The different steps are highlighted by large rectangles ranging from light to dark green.

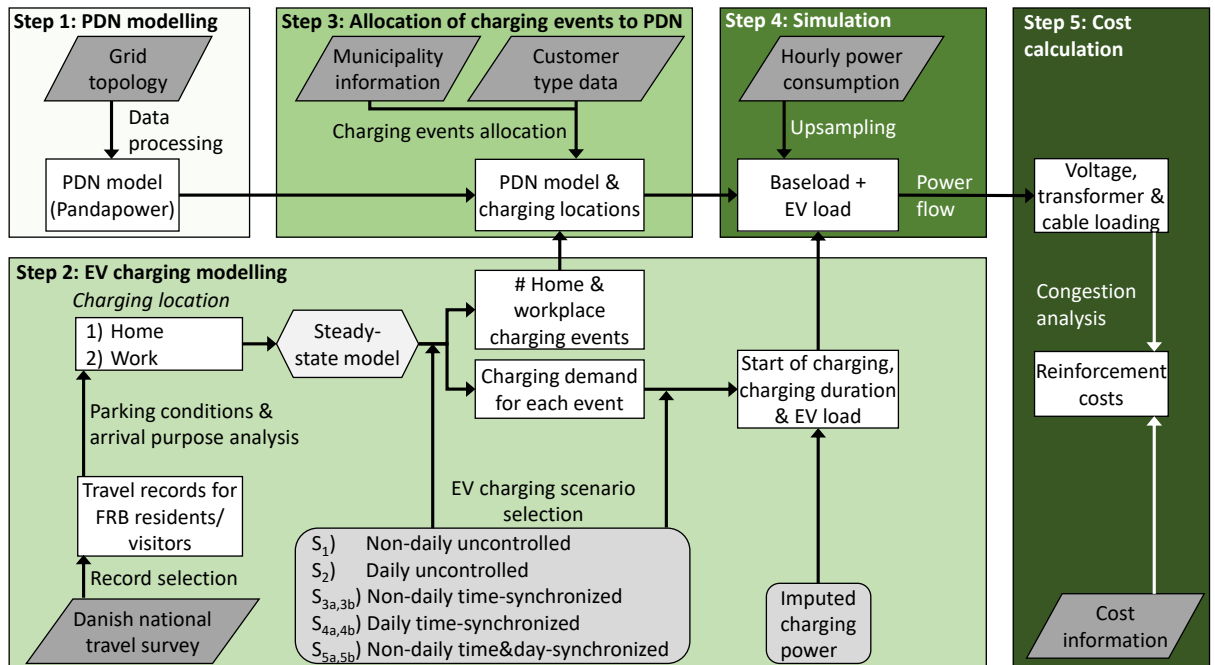


Figure 1: Methodology of the paper to derive the impact of different charging strategies on the power distribution network of Frederiksberg. While dark grey shaded rhomboids indicate the input data, grey shaded shapes represent the external parameter. The light grey shaded hexagon indicates external models [10] used in this work. White shaded rectangles illustrate results obtained in each step of the process.

## 2.1 Power distribution network modelling

The modelling software to analyse the PDN in Frederiksberg makes use of the Python package Pandapower. This package allows for a straightforward representation of the 10 kV PDN of Frederiksberg to simulate the power flow in the respective infrastructure. For the purpose of this paper, we focus the analysis on the 10/0.4 kV transformers and the respective feeding underground cables. The power grid network topology is defined based on data collected from the DSO for this area, Radius, which provided the location and characteristics of its transformers and respective cables. In normal operation, the PDN of Frederiksberg is divided into three independent networks, labelled  $FRBi$  with  $i=\{1, 2, 3\}$ , as depicted in Fig. 2. Each PDN has its own main station 30/10 kV coupled to multiple feeders connecting the respective transformers. Additional connections between the PDNs exist, which can be deployed as tie-lines to connect the transformers in contingency scenarios. In this work, we only consider normal operation in which the three PDNs are operated independently.

A brief description of the PDNs' main characteristics is given in Tab. 1, and the layout is illustrated in the left part of Fig. 2. In the right part of Fig. 2, we identify the areas of Frederiksberg that are primarily dedicated to workplace parking and private residential housing areas. It is worth noting the reduced density of transformers in areas associated with the latter. A detailed description of the mapping of home and workplace charging, based on the identified zones, is presented in Section 2.3. Both plots are shown on the footprint of Frederiksberg municipality, with grey lines indicating roads and walking paths, and buildings represented in light blue colour.

Table 1: Summary of the power distribution network infrastructure in Frederiksberg. For each  $FRBi$ , there are  $N_{tr}^i$  transformers, connected to  $N_c^i$  cables covering a total length  $L_c^i$  (km).

$FRBi$	$N_{tr}^i$	$N_c^i$	$L_c^i$ (km)
1	152	222	93.4
2	98	157	60.0
3	34	61	19.9

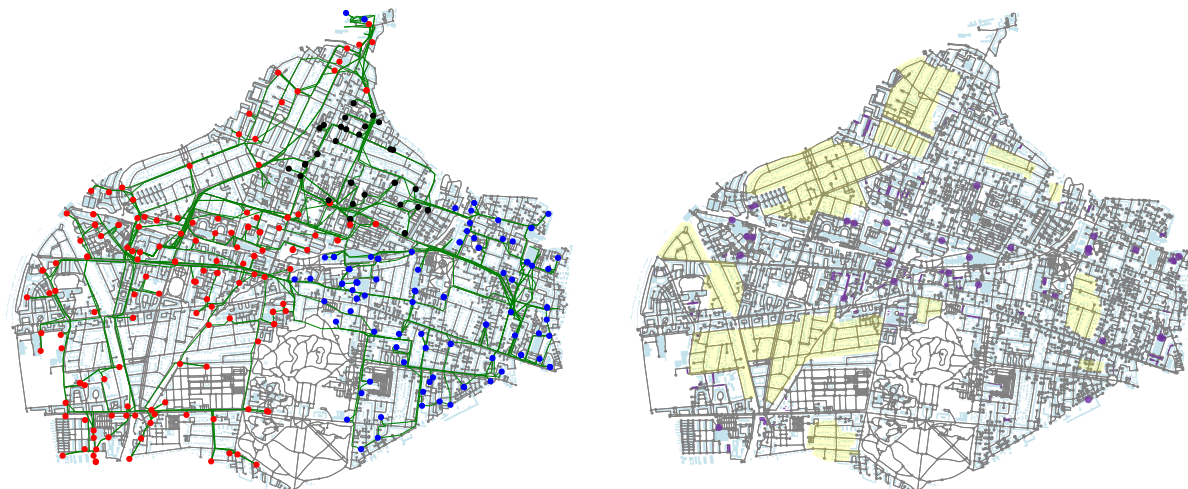


Figure 2: Visualization of the power distribution network topology (left) and distribution of zone types (right) in Frederiksberg. The 10/0.4 kV transformers are mapped to the respective PDN by colour coding, with red, blue, and black solid dots representing  $FRBi = \{1, 2, 3\}$  while the underground cables for all PDNs are shown in green. On the right, the residential housing areas with predominantly single-family/row houses are highlighted with a yellow shade and the primary workplace parking areas are represented in purple shade.

## 2.2 EV charging modelling

The evaluation of the daily EV demand is based on two pillars. Firstly, travel records (private car trips only) from the Danish national travel survey in the years 2006 – 2019 [13]. Secondly, on the models for the decision to charge and steady-state state-of-charge distributions introduced in Ref. [10].

From the travel survey, we collect all travel records for private car utilization that visit Frederiksberg at least once, which define a pool of donor of representative travel records. Since the travel survey

samples yearly a small fraction of the population, each record includes a calibration factor  $\lambda$  that ensures a representative picture of the population in each year. We make use of this calibration factor to generate an expanded pool of travel records, such that each donor record spawns  $\lfloor \lambda \rfloor$  records in the expanded pool. In this process, we utilize origin-destination traffic matrices to introduce random variation to the location of each activity in the expanded pool of records, while still preserving the traffic patterns. By making use of the information available, we characterize the records by home residency and workplace municipalities, the parking conditions and the type of day. The travel survey does not indicate the specific day for each record, rather it identifies the respective type of day. Normal weekdays, defined as Monday to Thursday where the next day is not a holiday or special day, comprise the bulk of the travel records, approximately 57.4% of all records. The next largest subset of records concerns Fridays or weekdays prior to holidays, accounting for approximately 14.6%. The remaining groups contain even smaller shares of donor pool, making these to susceptible to non-representative variations from outlier records. Therefore, we restrict our analysis to travel records from the largest group.

In addition, we leverage the data on parking conditions at home and work to identify the potential access to home and workplace charging, which we use to categorize the records into non-overlapping subgroups, as depicted in Fig. 3. Given the scarcity of records for EVs in the travel survey, we make use of records from vehicles with conventional drive-trains. For each record, we attribute a battery capacity based on a review of new EV specifications, assuming a fleet with a mean capacity of 68 kWh with a standard deviation of 18 kWh and set the mean rate of conversion for all records at  $\eta = 0.2$  kWh/km.

The models introduced in Ref. [10] are then used to determine the required energy to meet travel requirements  $\delta\epsilon$ , the probability of charging at a given day  $p_d$ , the mean interval between charging events  $d_p$ , as well as the steady-state demand for each charging scenario.

### 2.2.1 Classification of travel records

The distribution of the charging events is determined by a hierarchical filtering process, based on the parking conditions at home and work, as well as the travel diaries details, as depicted in Fig. 3. To begin with, we segregate the records according to the residency municipality to identify the share of charging events from residents and the demand emerging from visitors. The visitors comprise any person that at any point in their travel record drives into the selected municipality. Then, we start the hierarchical filtering process. First, we assess the parking conditions at home. For those with reliable access to parking at their premises or on/next to the property, we infer that home charging will be available to such drivers, i.e. parking conditions matching codes {4, 5, 6, 111, 112, 131, 132} in the travel survey [13]. If the travel records indicate that the vehicle returns home on that day, we attribute the demand from this record to *home* charging. Second, remaining records are then screened for parking conditions at work, namely work parking codes {1, 2, 3, 11, 12} [13]. By the same token, we attribute *workplace* charging if the travel records indicate a visit to the workplace on that day. Since the workplace municipality can be different from the residency, we account for the contribution inside and outside Frederiksberg. The remaining demand is assigned to charging using the public infrastructure and is exempt from our impact analysis within this work. It is worth noting that we are likely overestimating the penetration of home and workplace charging, by assuming that everyone who has conditions to have a charger, will install one. Hence, the results shown in this paper should be interpreted as upper bounds to the share of charging demand met at home and the workplace.

### 2.2.2 Energy demand

Even though the market share of EVs in Denmark remains low so far [14], for the purpose of this paper, we consider an ambitious scenario of full electrification of the private passenger cars fleet of the year 2020, i.e. 24252 cars [15]. Assuming a homogeneous distribution of EVs at the national level and present day traffic patterns, we should expect in this scenario that the total number of EVs transiting in Frederiksberg daily reaches  $N_t = N_r + N_v = 59070$ , where  $N_r = 24252$  and  $N_v = 34818$  are the number of EVs from residents and visitors, respectively. To ensure a representative load profile, we randomly sample travel records for each day in the power flow simulation, collecting  $N_r$  residents and  $N_v$  visitors. We collect travel records for 40 weekdays of peak loading, to be discussed in more detail in Section 2.4.

Based on this set of records, we run the five above-mentioned charging scenarios. In scenarios  $S_1$  and  $S_3$ , the number of charging events is determined by the probability  $p_d$  of each EV charging on a given day, as defined in Ref. [10]. For the purpose of this paper, we draw a random number from a uniform distribution in the interval  $r \in [0, 1]$  and define the acceptance criteria for the decision to charge as  $r \leq p_d$ . Consequently, the number of charging events in said scenarios is stochastic in nature and smaller than the number of events in the remaining scenarios. Conversely, in the remaining scenarios, we observe as many charging events as records matching the filtering criteria depicted in Fig. 3.

A summary of the maximum number of home  $N_H$  and workplace  $N_W$  charging events and the respective charged energy is presented in Tab. 2, where the total charging demand for  $j$  charging events at the location  $X$  for  $S_1, S_3, S_5$  is defined as  $E_X = \sum_j \delta\epsilon_j$  and for  $S_2$  and  $S_4$  as  $E_X = \sum_j \delta\epsilon_j / d_p$ .

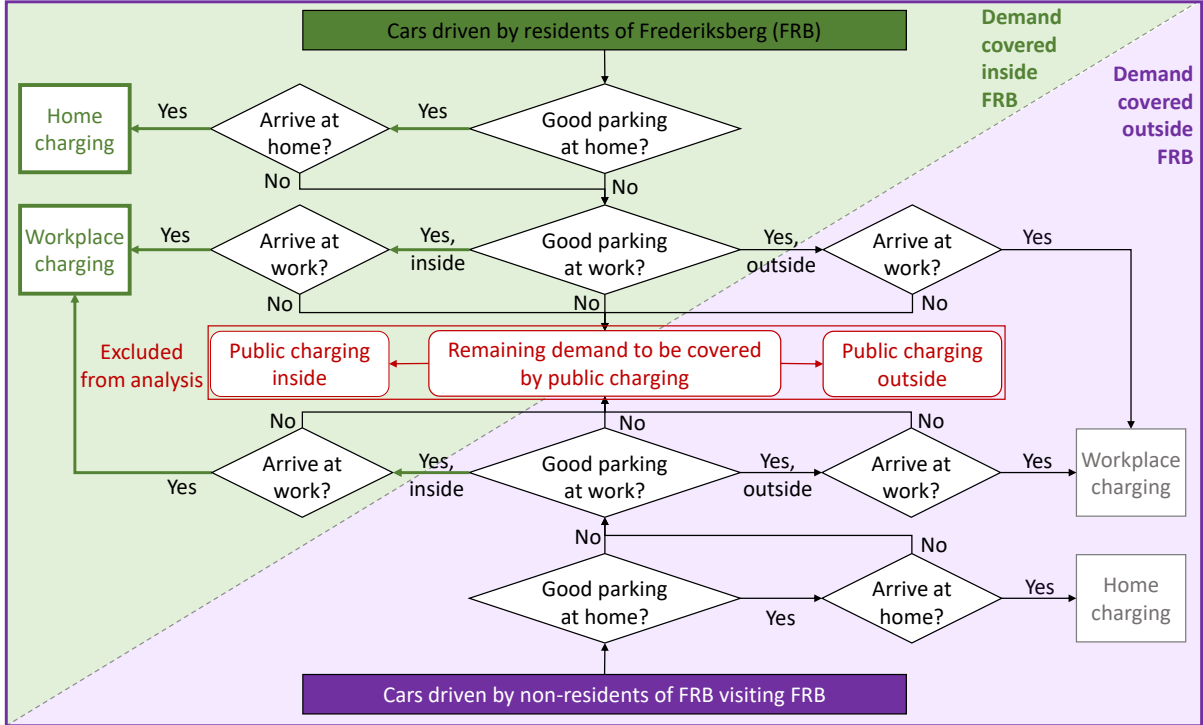


Figure 3: Representation of the segmentation of travel records according to residency and workplace municipality, as well as the parking conditions at the respective locations.

Table 2: Maximum number of charging events and respective energy demand per day during the simulation time span. Results are segregated by home and workplace charging for each scenario under consideration.

	$S_1$	$S_2$	$S_3$	$S_4$	$S_5$
$N_H$	2793	12686	2793	12686	12686
$N_W$	867	3089	867	3089	3089
$E_H$ (MWh)	68.4	81.2	68.4	81.2	350.5
$E_W$ (MWh)	21.2	26.1	21.2	26.1	83.4

Having identified the EV demand and number of charging events for each scenario, we will now focus our attention on the simulation of the charging events.

### 2.2.3 Simulation of charging events

In this paper, we are interested in the power grid impact of normal AC charging. Recently released EV models are converging towards supporting 11 kW AC charging, in line with the most common configuration of normal charging stations in Denmark. We frame our analysis assuming a large EV fleet capable of fully utilizing this type of infrastructure. Hence, throughout this paper we consider the charging power to be 11 kW, regardless of the scenario under analysis and the EV's state-of-charge. Therefore, the charging duration is determined by dividing the required energy by the constant charging power.

Given the daily variation of demand on the PDN, we consider different scenarios for smart charging according to a broadcasting control signal or a common objective. For home charging, we consider two sub-scenarios, namely *a* and *b*. In sub-scenario *a* the control signal delays the start of charging until midnight, i.e. 24:00 (00:00 of the next day), whereas sub-scenario *b* delays charging until 18:00. During working hours, we consider only one synchronization control signal that takes place at 10:00 and affects only vehicles charging at the workplace. Therefore, the start of charging at a location  $X$  is defined as  $t_{s,X} = \max(t_{c,X}, t_{a,X})$ , where  $t_{c,X}$  is the synchronization control signal time (for uncontrolled charging in  $S_1$  and  $S_2$  we set  $t_{c,X} = 00:00$ ) and  $t_{a,X}$  is the arrival time at the location. When travel records include multiple visits to home or workplace, we select the arrival time as follows: for home charging we consider the last arrival, whereas for workplace we take the first. Vehicles visiting the home location during the day, but not terminating the day at home, are exempted from the synchronization and start

charging immediately upon arrival.

Regarding smart charging, we consider two strategies. The first encompasses the synchronization of charging to a specific time of the day, where the decision to charge is stochastic for  $S_3$ , based on the probability of charging  $p_d$ , and forced to daily charging in  $S_4$ . The second strategy concerns synchronization of charging to a specific day and time, where we consider all records regardless of  $p_d$ . The strategies are labelled as T.S. for time-synchronized and as T.D.S for time- and day-synchronized, with the latter being used in  $S_5$  only. A final set of labels is introduced to distinguish home from workplace charging strategies, namely  $H_i$  and  $W_i$ , as the sub-scenarios  $a$  and  $b$  only apply to home charging. A summary of the configuration of each scenario can be found in Tab. 3. Charging events are simulated over a period of 24h in 15 min resolution starting at 05:00 on the given day to be able to both capture early charging at work and late charging at home without compromising capturing the majority of EV demand throughout one day. Furthermore, it is worth noting that some records encompasses parking durations that are insufficient to fully charge the EV. While scarce and mostly affecting workplace charging, our simulations force vehicles to complete charging.

Table 3: Summary of the characteristics of each charging scenario  $S_i$ , including sub-scenarios  $a$  and  $b$ , as well as  $H_i$  and  $W_i$ . The non-daily (n.d.) charging demand  $\delta\varepsilon$  is defined as the required energy according to the steady-state model, whereas the daily demand is  $\delta\varepsilon/d_p$  as introduced in the definition of  $S_i$ .

	$S_1$ $H_1, W_1$	$S_2$ $H_2, W_2$	$S_{3a}$ $H_{3a}, W_3$	$S_{3b}$ $H_{3b}, W_3$	$S_{4a}$ $H_{4a}, W_4$	$S_{4b}$ $H_{4b}, W_4$	$S_{5a}$ $H_{5a}, W_5$	$S_{5b}$ $H_{5b}, W_5$
pattern	n.d.	daily	n.d.	n.d.	daily	daily	n.d.	n.d.
control	none	none	T.S.	T.S.	T.S.	T.S.	T.D.S.	T.D.S.
$t_{c,H}$	none	none	24:00	18:00	24:00	18:00	24:00	18:00
$t_{c,W}$	none	none	10:00	10:00	10:00	10:00	10:00	10:00

### 2.3 Allocation of charging events to the power distribution network

Having modelled the PDN topology as discussed in Section 2.1 with its tripartite nature, we now have to allocate the charging events to the different transformers. The PDNs under consideration contain multiple classes of transformers, ranging from public to private (owned by consumers) and finally reserve. For the purpose of our simulations, we only allocate charging events to transformers from the public infrastructure. The remaining transformers are accounted for in the simulation, but no additional EV load is added. The distribution of charging events also accounts for the type of housing associated with home charging, such that private home charging is mapped to single-family/row house infrastructure and shared home charging is associated with denser housing infrastructure, e.g. apartment blocks.

The allocation procedure can be summarized in four broad steps. First, we divide home charging events according to the type of charging infrastructure used, i.e. private or shared. Based on customer type data provided by the DSO, we infer that the number of daily private home charging events during one day in  $S_2$ ,  $S_4$ , and  $S_5$  equates roughly to 80% of the total number of detached houses in Frederiksberg, from which we derive the ratio between private and shared home charging. For  $S_1$  and  $S_3$  the number of private home charging events is reduced by the ratio between the total number of home charging events in  $S_2$ ,  $S_4$ , and  $S_5$  and the total number of home charging events in  $S_1$  and  $S_3$ . In the second step, we consider the allocation of private home charging events. The respective charging events are distributed to the transformers that supply residential zones with predominantly single-family or row houses. This attribution is based on the overlap of single-family housing zones (including a vicinity buffer) and the location of the transformers, with the number of events being proportional to the relative size of the respective housing zone. The third step concerns the allocation of shared home charging. The amount of charging events for shared charging is calculated as the difference between total and private home charging events. These are then equally distributed to all transformers, that do not supply aforementioned single-family housing zones. The fourth step handles the allocation of the load from workplace charging. It begins with the identification of transformers that can supply this load, based on the locations of workplace parking lots near company or institution offices and other intensive labour locations. This part of the procedure relies on public data collected from OpenStreetMap. Workplace charging events are then allocated to the nearest transformers using the shortest path between the transformer and respective location, according to the real road and public walking paths in Frederiksberg. Finally, it is important to note that the allocation procedure has to be repeated for each simulation scenario and simulated day, as the number of charging events is dependent on the configuration of each scenario and sampled records. A summary of the maximum number of charging events allocated to each of the three PDNs is depicted in Tab. 4. In addition, we observe that the amount of charging events allocated to a single transformer in scenarios  $S_1$  and  $S_3$  lies in the following ranges: 2 to 25 for private home, 11 to 12 for shared home, and 18 to 19 for workplace charging events. In scenarios  $S_2$ ,  $S_4$  and  $S_5$  the number of events increases considerably, but private home continues to exhibit the largest interval and shared and workplace exhibit

minimal variation as in the other scenarios. The respective ranges read: 11 to 108 private home, 51 to 52 shared home, and 65 to 66 workplace charging events.

Table 4: Summary of charging events allocation in the FRBi networks. We list the maximum number of events allocated to private home  $N_{H,p}^{(i)}$ , shared home  $N_{H,sh}^{(i)}$  and workplace  $N_W^{(i)}$  charging.

	$N_{H,p}^{(1)}$	$N_{H,sh}^{(1)}$	$N_W^{(1)}$	$N_{H,p}^{(2)}$	$N_{H,sh}^{(2)}$	$N_W^{(2)}$	$N_{H,p}^{(3)}$	$N_{H,sh}^{(3)}$	$N_W^{(3)}$
$S_1, S_{3a} - S_{3b}$	275	1312	480	21	821	313	11	353	74
$S_2, S_{4a} - S_{5b}$	1244	5953	1710	95	3734	1116	54	1606	263

## 2.4 Power flow simulation and reinforcement cost calculation

The power flow simulation is a computationally demanding problem to solve. Since the PDN needs to be properly dimensioned for the days of highest loading, we make use of the provided power consumption data of the year 2020 to select all days in which at least one transformer experience its maximum loading. Based on this criterion, we identify a total number of 67 days of high load, which fall within the periods Jan-Mar and Aug-Dec. Furthermore, as discussed in Section 2.2, we consider only normal weekdays, by this token the size of the identified pool is further reduced to 40. By focusing on this reduced sample, we are able to effectively reduce the computational load and analyse multiple EV charging scenarios.

To be able to assess the EV impact on the PDNs, both in terms of voltage deviations and transformer and cable overloading, the provided baseload and estimated EV load are aggregated for each transformer within the networks. The baseload data for each transformer is only available in hourly resolution. Hence, we make use of cubic interpolation to infer the load in a 15 min timescale. Moreover, as previously mentioned, the EV demand is modelled for a period of 24h starting at 05:00 on the given day of peak load. Thus, the baseload of the PDNs is chosen accordingly within the same period. While the baseload varies according to the day, the estimated EV load also exhibits variation for each day due to the sampling, as discussed in each Section 2.2. It is worth noting that the reactive power of EV charging is neglected within this work. Finally, the Newton-Raphson method is used for the power flow simulation of each selected day in 15-min resolution.

To assess the reinforcements cost associated with the overloading of transformer and cables observed in our simulations, we assume a typical cost of 133 k€/km for cable and 21.64 k€ for transformer replacements, as used in Refs. [16, 17].

## 3 Results

Having discussed the methodology of the paper, this section is dedicated to the main results of our work. Here, we address the findings for both the EV and aggregated demand, as well as the power flow simulation.

### 3.1 EV demand and aggregated power consumption

To begin with, we focus on the estimated EV demand and aggregated power consumption for Frederiksberg. This estimate serves as an input to the power flow simulations. Fig. 4 illustrates the aggregated EV demand over the course of 24h and associated CF, defined as the ratio of the simultaneous maximum demand over the maximum demand capacity of EVs using home and workplace charging, respectively. By comparing home charging scenarios *a* and *b*, it can be seen that charging synchronization at midnight leads to a significant higher peak load compared to synchronizing at 18:00, as the majority of EVs arrived at home and charge at the same time. While for *a* a maximum CF of 94.8% is observed, this decreases significantly to 58.7% in *b*, with a similar variation in the maximum peak power demand, respectively 131.7 and 81.6 MW. Furthermore, the time of synchronization also has an impact on the magnitude of experienced peak load between  $S_4$  and  $S_5$ . While synchronization at midnight leads to similar peak loads in both scenarios, the peak load in  $S_5$  is notable higher when considering synchronization time 18:00 due to longer charging durations. A summary of the time and scale of maximum peak load and maximum CF is provided in Tab. 5. Comparing the results to existing literature, the CF in  $H_1$  and  $H_{4a}$  is similar to results from Ref. [6], which estimates the CF of a fleet of 10000 EVs to be 9% for non-daily uncontrolled charging, and 83% for daily price-responsive charging starting at 22:00.

The aggregated apparent power demand for Frederiksberg is illustrated in Fig. 5. For scenarios  $S_1 - S_3$ , an increase in peak load of less than 32% is experienced. In contrast, the peak load increases by roughly 183%, 100%, 215% and 157% in  $S_{4a}$ ,  $S_{4b}$ ,  $S_{5a}$  and  $S_{5b}$  respectively. Thus, charging synchronization of a large fleet of EVs at midnight could cause higher concerns compared to the synchronization at 18:00 where the EV load coincides with the baseload of the system.

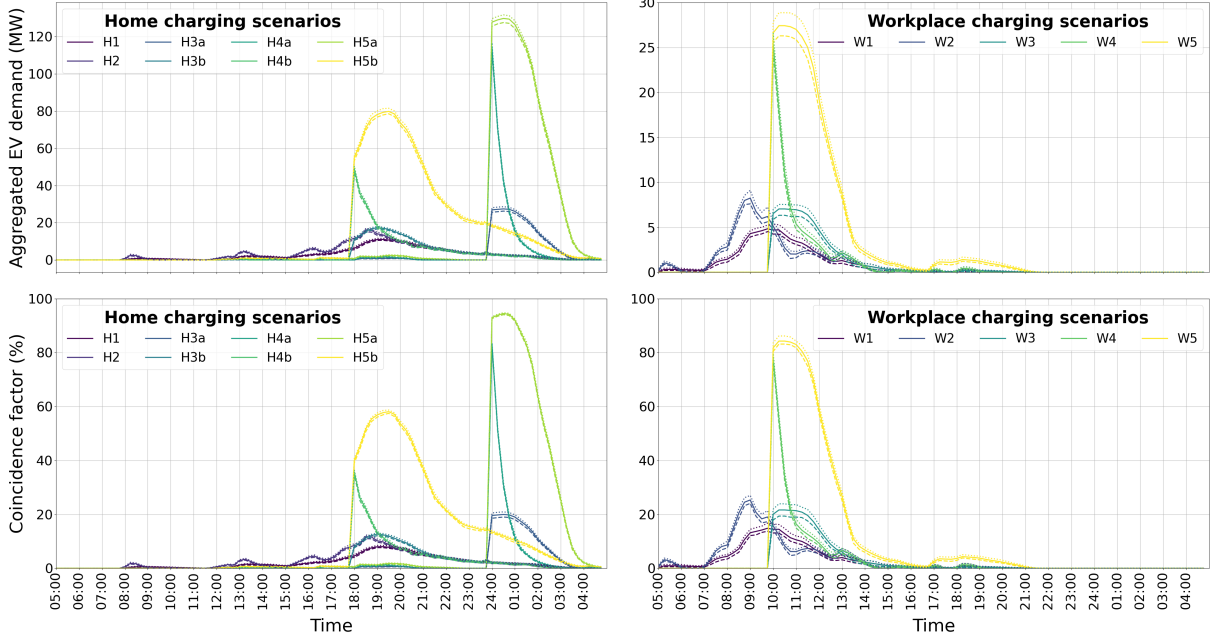


Figure 4: Overview of the aggregated EV demand at home (upper left) and work (lower left), and the coincidence factor of home (upper right) and workplace charging (lower right) for each charging scenario. Average, minimum, and maximum values for the 40 demand profiles are illustrated by solid, dashed and dotted lines respectively.

Table 5: Summary of the aggregated EV peak power demand for each charging scenario, decomposed according to home and workplace contributions. We list its magnitude  $P_{\max}$ , time  $t_{\max}$ , and coincidence factor  $CF_{\max}$ .

	$P_{\max}$ (MW)	$t_{\max}$	$CF_{\max}$ (%)
$H_1$	11.6	19:15	8.5
$H_2$	16.9	18:30	12.4
$H_{3a}$	28.6	00:30	21.0
$H_{3b}$	18.0	19:00	13.1
$H_{4a}$	116.8	24:00	83.7
$H_{4b}$	50.4	18:00	36.5
$H_{5a}$	131.7	00:30	94.8
$H_{5b}$	81.6	19:30	58.7
$W_1$	5.3	10:00	16.8
$W_2$	9.1	09:00	27.0
$W_3$	7.6	10:15	23.9
$W_4$	26.6	10:00	79.8
$W_5$	28.9	10:15	86.2

### 3.2 Power distribution network impact and reinforcement costs

The EV impact on the PDNs of Frederiksberg is evaluated with respect to bus voltages and the loading of transformers and underground cables. The replacement of PDN's components is a time-consuming process, and thus it is important for DSO planners to look at components that could potentially face congestions in the future to be able to make timely decision regarding network reinforcements. To analyse the loading of components, two thresholds are considered, namely 75% and 100%. A summary of the total number of transformers and cables loaded above 75% and 100%, as well as the respective cable length and the estimated reinforcement costs, is shown in Tab. 6. Voltage violations are not experienced in any of the simulated scenarios and are thus not further addressed in this section. Comparing the loading of transformers and cables, it can be seen that transformer overloading is more prominent. For  $S_1 - S_{3b}$  no cable overloads are recorded and a maximum of two transformers experience overload situations. For the extreme scenarios  $S_4$  and  $S_5$ , a notable number of transformers and cables experience congestions. Compared to home charging synchronization at 18:00 (b), synchronization at midnight (a) exerts a sig-

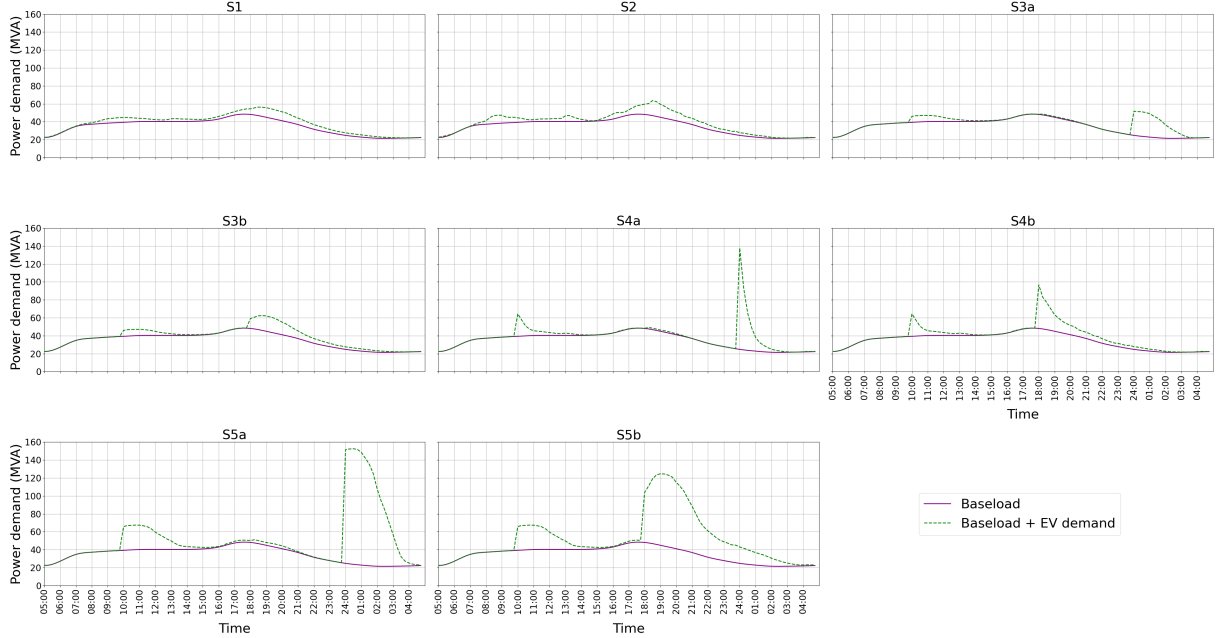


Figure 5: Aggregated apparent power demand of all three power distribution networks in Frederiksberg. The purple plot indicates the aggregated baseload from 05:00 on 2020-01-06 to 04:45 on 2020-01-07. The green dashed plot illustrates the aggregated demand of baseload and EV demand for each charging scenario.

nificant higher impact on the PDNs both in terms of transformer and cable overloading, indicated by a significant increase in reinforcement costs.

Table 6: Summary of reinforcement costs required to match the increased load in each scenario  $S_i$ . We indicate the number of transformers  $n_{tr} \equiv n_{tr}^1, n_{tr}^2, n_{tr}^3$ , cables  $n_c \equiv n_c^1, n_c^2, n_c^3$ , and total cable length  $l_c \equiv l_c^1, l_c^2, l_c^3$  (km) per PDN in Frederiksberg that exhibits load exceeding 75% and 100% of the nominal load. The last column contains an estimate for the total cost  $C_T$  (k€) associated with the respective reinforcement.

Load (%)	$n_{tr}$		$n_c$		$l_c$ (km)		$C_T$ (k€)	
	>75	> 100	> 75	> 100	>75	> 100	>75	> 100
$S_1$	5, 1, 0	1, 0, 0	0, 0, 0	0, 0, 0	0, 0, 0	0, 0, 0	130	22
$S_2$	12, 7, 0	1, 1, 0	0, 0, 0	0, 0, 0	0, 0, 0	0, 0, 0	411	43
$S_{3a}$	6, 2, 0	1, 0, 0	0, 0, 0	0, 0, 0	0, 0, 0	0, 0, 0	173	22
$S_{3b}$	7, 2, 0	1, 0, 0	0, 0, 0	0, 0, 0	0, 0, 0	0, 0, 0	195	22
$S_{4a}$	120, 69, 32	59, 40, 9	32, 9, 0	16, 3, 0	16.5, 5.3, 0	8, 2.1, 0	7676	3680
$S_{4b}$	74, 52, 14	34, 21, 4	12, 2, 0	2, 0, 0	5.1, 1.3, 0	0.4, 0, 0	3878	1333
$S_{5a}$	122, 69, 32	86, 67, 25	34, 13, 0	19, 4, 0	17.6, 7.1, 0	9.2, 3.3, 0	8103	5509
$S_{5b}$	112, 69, 32	54, 38, 8	21, 9, 0	11, 2, 0	10.1, 5.3, 0	4.9, 1.3, 0	6656	2983

To showcase the impact of home and workplace charging, we illustrate in Fig. 6 the loading of four different transformers in Frederiksberg over the course of 24h, starting at 05:00 on 2020-01-06. Here, we consider four different examples, starting with no overloading in any scenario (upper left). Examples of overloading cause by either home or workplace charging are shown in the bottom left and right plots. Finally, an example of both workplace and home charging causing overloading is depicted in the upper right plot. Thus, even though the home charging demand is estimated to be significant higher than the workplace charging demand, synchronized charging at work also contributes to potential congestions.

## 4 Discussion

Results indicate that even if full EV penetration is reached, uncontrolled charging is not likely to cause a significant challenge to the urban PDNs of Frederiksberg. The worst-case scenarios,  $S_4$  and  $S_5$  (and

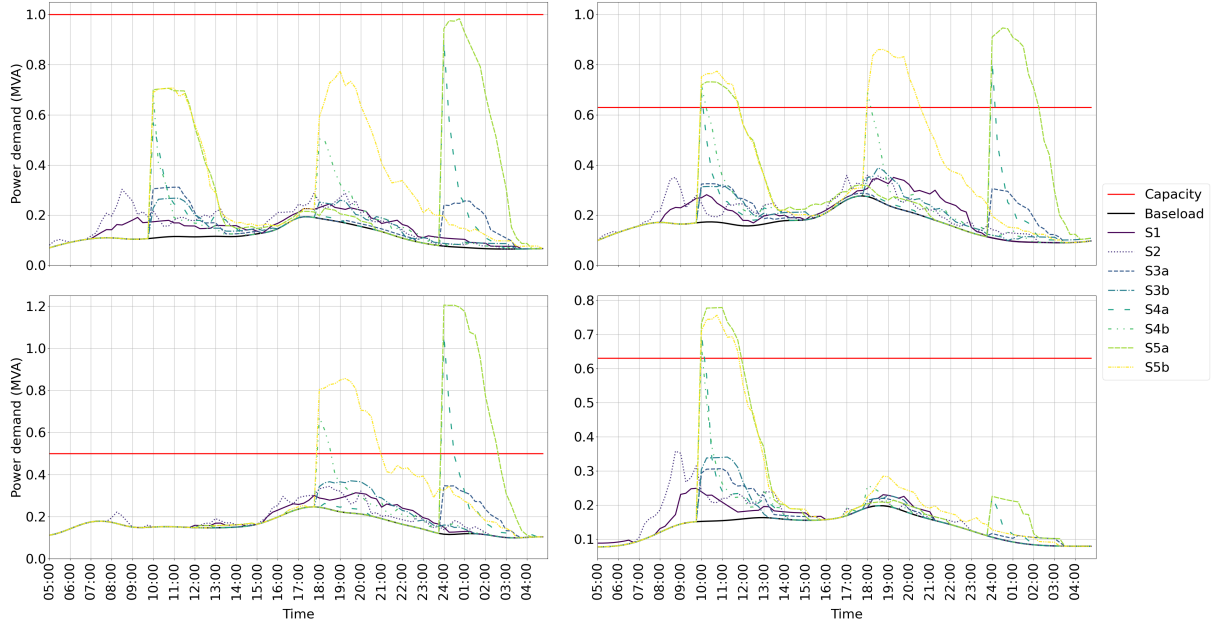


Figure 6: Transformer loading of four different 10/0.4 kV transformers in Frederiksberg from 2020-01-06 05:00 to 2020-01-07 04:45. While the red line indicates the capacity threshold of each transformer, the black line illustrates the baseload. Coloured lines in different shapes indicate the aggregated apparent power demand (Baseload + EV demand) in each scenario.

respective sub-scenarios), while rare and unlikely, should be taken into consideration if no dampening mechanisms are introduced to curb excessive demand surges. However, several factors not taken into account within this work could have a significant impact, that can either reduce or aggravate the load on the PDN.

Concerning the former, the scenarios introduced in this paper represent extremes both in terms of charging patterns and control, as well as in terms of the availability of home and workplace charging. Therefore, results should be taken as illustrative upper bounds for the expected impact on the grid. Regarding the charging pattern, each charging scenario assumes the same charging behaviour for all EV users. However, in reality charging behaviour is complex in nature, involves multiple patterns (e.g. daily *vs.* non-daily), is subject to different control strategies (e.g. uncontrolled *vs.* smart-charging), and variable charging power is likely a critical element. On top of this, future market products offered by charging operators could add another dimension of complexity by offering potential financial benefits to the customers. Regarding charger installation, we assume throughout this paper that all EV owners with access to good parking conditions, either at home or work, will have access to a charger, which could lead to overestimating the number of users with access to charging at those locations. Furthermore, workplace and housing associations are prime candidates for the utilisation of load sharing solutions in their charging infrastructure, which should naturally dampen high-demand surges. Last but not least, constraints in the low voltage PDN may also dampen the impact on the medium voltage PDN, i.e. bottlenecks might materialize on the low voltage level before any congestions are experienced on the medium voltage level. In contrast to the above-mentioned factors that will likely dampen demand, we now delve into four factors that can aggravate demand. First, our simulations are based on present-day numbers of vehicles and driven distance, which fails to account for the likely growth of number of private cars, as expected by the Danish authorities [18]. Second, given the constraints associated with travel records, we assess the impact of EV charging on the grid based only on normal weekdays data, which covers the days when high synchronization is most likely to occur. Yet, it is important to note, that high demand could also occur during weekends or holidays. Third, the impact of public charging is not considered in the present study. Even in the least impactful scenario of evenly distributed utilization of public charging this will add additional load to the power grid. The fourth factor concerns the spatial dispersion of charging infrastructure and respective connections to the PDN. As previously discussed, the likelihood of global synchronization of demand on the entire grid is rather low. Yet, congestion could also arise from excessive concentration of charging in areas with limited number of transformers and reduced cable connections, leading to hotspots of demand that could locally overload the power grid.

## 5 Conclusion

This paper probes the impact of full electrification of private vehicle utilization on the urban medium voltage PDN of Frederiksberg (Denmark), both in terms of transformer and cable loading, as well as voltage deviations. Making use of Danish travel survey data, we estimate the future EV demand for home and workplace charging, that will have to be served by the PDN. To identify potential congestions in the PDN, we devise five different charging strategies comprising different charging patterns and degrees of control. We simulate the impact of each charging scenario on top of the present base load, selecting 40 weekdays of peak loading within the system. Three of the five charging scenarios focus on highly coordinated start of charging to account for a potential high level of charging synchronization in the future when applying smart charging to achieve a certain objective.

The results indicate that transformer overloading is the primary concern for the analysed PDN, with cable overloading being less prominent and no detected voltage violations. Moreover, uncontrolled charging does not pose a massive concern for the PDN, mostly due to a low coincidence factor of charging. Furthermore, even with high charging synchronization, no severe impacts are to be expected when EVs are not charged on a daily basis. However, rare events involving either time-synchronization for daily charging patterns, or day- and time-synchronization for non-daily charging patterns could stress the grid and lead to severe overloading of transformers. Finally, due to a higher coincidence factor of home charging at midnight, synchronization during the night could potentially pose a bigger challenge to PDNs compared to the synchronization at peak loading times in the evening.

Our future work will focus on analysing the impact on the low voltage PDN, which may be subject to more significant challenges from electric vehicle synchronization, especially with regard to home charging.

## Acknowledgments

The work in this paper has been supported by the research project FUSE (EUDP grant nr. 64020-1092). Website: <http://www.fuse-project.dk>. Furthermore, we would like to thank the DSO Radius for providing the data for this work.

## References

- [1] P. Wolfram and N. Lutsey, “Electric vehicles: Literature review of technology costs and carbon emissions,” *The International Council on Clean Transportation: Washington, DC, USA*, pp. 1–23, 2016.
- [2] L. Calearo, A. Thingvad, K. Suzuki, and M. Marinelli, “Grid Loading Due to EV Charging Profiles Based on Pseudo-Real Driving Pattern and User Behavior,” *IEEE Transactions on Transportation Electrification*, vol. 5, no. 3, pp. 683–694, 2019.
- [3] E. Veldman and R. A. Verzijlbergh, “Distribution grid impacts of smart electric vehicle charging from different perspectives,” *IEEE Transactions on Smart Grid*, vol. 6, no. 1, pp. 333–342, 2014.
- [4] C. Crozier, T. Morstyn, and M. McCulloch, “The opportunity for smart charging to mitigate the impact of electric vehicles on transmission and distribution systems,” *Applied Energy*, vol. 268, p. 114973, jun 2020.
- [5] J. Bollerslev, P. B. Andersen, T. V. Jensen, M. Marinelli, A. Thingvad, L. Calearo, and T. Weckesser, “Coincidence factors for domestic ev charging from driving and plug-in behavior,” *IEEE Transactions on Transportation Electrification*, vol. 8, no. 1, pp. 808–819, 2022.
- [6] F. Gonzalez Venegas, M. Petit, and Y. Perez, “Plug-in behavior of electric vehicles users: Insights from a large-scale trial and impacts for grid integration studies,” *eTransportation*, vol. 10, p. 100131, 2021. [Online]. Available: <https://www.sciencedirect.com/science/article/pii/S2590116821000291>
- [7] A. S. B. Humayd and K. Bhattacharya, “A novel framework for evaluating maximum pev penetration into distribution systems,” *IEEE Transactions on Smart Grid*, vol. 9, no. 4, pp. 2741–2751, 2018.
- [8] R. A. Verzijlbergh, L. J. De Vries, and Z. Lukszo, “Renewable energy sources and responsive demand. do we need congestion management in the distribution grid?” *IEEE Transactions on Power Systems*, vol. 29, no. 5, pp. 2119–2128, 2014.
- [9] N. Sadeghianpourhamami, N. Refa, M. Strobbe, and C. Develder, “Quantitive analysis of electric vehicle flexibility: A data-driven approach,” *International Journal of Electrical Power & Energy Systems*, vol. 95, pp. 451–462, 2018.

- [10] F. Hipolito, C. Vandet, and J. Rich, “Charging, steady-state soc and energy storage distributions for ev fleets,” *Applied Energy*, vol. 317, p. 119065, 2022. [Online]. Available: <https://www.sciencedirect.com/science/article/pii/S0306261922004597>
- [11] “FUSE - Frederiksberg Urban Smart Electromobility,” <http://www.fuse-project.dk>, accessed: 2022-03-31.
- [12] T. Unterluggauer, J. Rich, P. B. Andersen, and S. Hashemi, “Electric vehicle charging infrastructure planning for integrated transportation and power distribution networks: A review,” *eTransportation*, vol. 12, p. 100163, 2022. [Online]. Available: <https://www.sciencedirect.com/science/article/pii/S2590116822000091>
- [13] O. Baescu and H. Christiansen, “The Danish National Travel Survey Annual Statistical Report TU0619v2,” Tech. Rep., 2020. [Online]. Available: <https://doi.org/10.11581/dtu:00000034>
- [14] Danmarks Statistik, “BIL54: Bestand af motorkøretøjer efter brugerforhold, køretøjstype, område, drivmiddel og tid,” 2021. [Online]. Available: [www.statistikbanken.dk/BIL54](http://www.statistikbanken.dk/BIL54)
- [15] D. Statistik, “Bil707: Bestanden af køretøjer pr 1 januar efter område og køretøjstype,” <https://www.statistikbanken.dk/bil707>, accessed: 2022-03-31.
- [16] S. Klyapovskiy, S. You, A. Michiorri, G. Kariniotakis, and H. W. Bindner, “Incorporating flexibility options into distribution grid reinforcement planning: A techno-economic framework approach,” *Applied Energy*, vol. 254, p. 113662, 2019.
- [17] S. Klyapovskiy, S. You, H. Cai, and H. W. Bindner, “Incorporate flexibility in distribution grid planning through a framework solution,” *International Journal of Electrical Power & Energy Systems*, vol. 111, pp. 66–78, 2019.
- [18] Finansministeriet, “Grøn skattereform Aftale om Grøn skattereform,” Tech. Rep., december 2020. [Online]. Available: <https://fm.dk/nyheder/nyhedsarkiv/2020/december/bred-aftale-om-groen-skattereform-baner-vej-for-groen-omstilling-i-erhvervslivet/>

## Presenter Biography



Tim Unterluggauer received his B.Sc. and M.Sc. degree in Industrial Engineering with a focus on the management of power grids from TU Dortmund University in 2018 and 2020 respectively. He is currently pursuing his Ph.D. degree with the Department for Wind and Energy Systems at Technical University of Denmark, Copenhagen, Denmark. His research interests include sustainable energy systems and electric vehicle integration into power grids.